Cost-Optimized Mooring Systems integrating Load Reduction Device for 15 MW FOWT

Salvatore Verde [1], Alverlando R. Silva[1], Eduardo N. Lages[2]

[1] *Campus do Sertão, Universidade Federal de Alagoas*
Rodovia AL 145, km 3, n⁰3849, CEP 57480-000, Delmiro Gouveia-AL, Brazil
alverlando.ricardo@delmiro.ufal.br, salvatore.verde@delmiro.ufal.br
[2] *Laboratório de Computação Científica e Visualização, Centro de Tecnologia, Universidade Federal de Alagoas, Av. Lourival Melo Mota, S/N, Tabuleiro do Martins, CEP 57072-970, Maceió-AL, Brazil*
enl@lccv.ufal.br

Abstract. The wind energy sector is shifting towards larger turbines to reduce energy costs, posing challenges for installations in shallow and intermediate waters (60-150 meters) that require smaller platforms and mooring systems. Previous research utilized a multi-objective optimization (MO) framework, employing tools like NSGA2 and OpenFast with MoorDyn, to design systems compatible with synthetic lines. Incorporating load reduction devices (LDRs) in mooring systems offers significant benefits by reducing loads on anchors and mooring lines, allowing for smaller, lighter anchors, and mitigating fatigue damage. LDRs, such as ballasted pendulums, polymer springs, and hydraulic dampers, feature unique non-linear stiffness curves crucial for performance. This study advances the MO framework by assessing a mooring system with spring polymer LDRs and conducting a sensitivity analysis of key design variables using the design of experiments (DOE) approach. It integrates the Pymoo optimization library with industrial software like OrcaFlex and OrcaWave, promoting broader industry adoption. The findings indicate significant reductions in mooring system costs, particularly for smaller mooring radii, and a 22% decrease in computational costs with fewer design variables, enhancing the mooring design process for any floating platform in any water depth.

Keywords: Floating wind turbine, Mooring systems, Nylon rope, Optimization, Spring Polymer

1 Introduction

The renewable energy sector is rapidly advancing into open seas with floating offshore wind technology. Governments aim for net zero emissions by the 2050s and 2060s, emphasizing wind energy's crucial role in environmental efforts. Currently, offshore wind capacity stands at 64.3 GW, accounting for 7% of the global total. GWEC Market Intelligence [1] forecasts an addition of over 380 GW by 2032, raising total capacity to 447 GW. Brazil's Offshore Support System (OSS) [2] manages offshore areas for power generation, with an estimated potential of 700 GW in shallow waters [3]. Despite growing turbine sizes, adapting mooring systems to shallow waters remains challenging [4]. Studies suggest synthetic ropes can reduce peak loads and CAPEX [4], [5], [6]. Loading reduction devices (LRDs) also show potential for CAPEX reduction [7], [8]. Optimization methods for mooring systems include frequency domain analysis [9], [10], metamodel techniques [11], and direct time-domain simulations [12]. A recent tiered constraint screening method for a multi-objective optimization genetic algorithm (MOGA) aims to achieve cost-effective mooring designs using OpenFast [13] and MoorDyn [14] with nylon and chain [6], [15]. However, literature lacks studies using preliminary sensitivity analysis of design variables, commercial software, and automated cost optimization for mooring systems with LRDs. This paper addresses these gaps by using the design of experiment approach to identify the most influential design variables and employing MOGA and OrcaFlex to optimize a mooring system with a spring polymer LRD. Polymer springs serve as versatile components in mooring lines. McEvoy and Kim [16] utilized them for floating tidal devices. Further insights, including cost-benefit analyses for FOWT mooring systems, are provided by Aryawan et al. [7], Lozon et al. [8], and McEvoy, Johnston and Marine [17] . These studies demonstrate that polymer springs reduce peak mooring loads and offer advantages such as improved fatigue life, reduced mooring footprint, and optimized platform motion. This paper examines a spring design with a degressive axial stiffness response curve, as shown in Fig.1, which also highlights the benefits of using this spring, designed to be stiff at lower tension levels and compliant with the turbine's thrust load. The outcomes in this paper were derived using a laptop with a 6-core CPU, 16 GB RAM, and a 237 GB SSD. The analysis used OrcaFlex and OrcaWave for offshore dynamic and diffraction analysis, pyDOE for sensitivity analysis, Pymoo for NSGA2 optimization, Scipy for Savitzky-Golay filtering, Openturns for generating the Generalized Extreme Distribution, Joblib for parallel computation, and Numpy and Panda for other tasks.

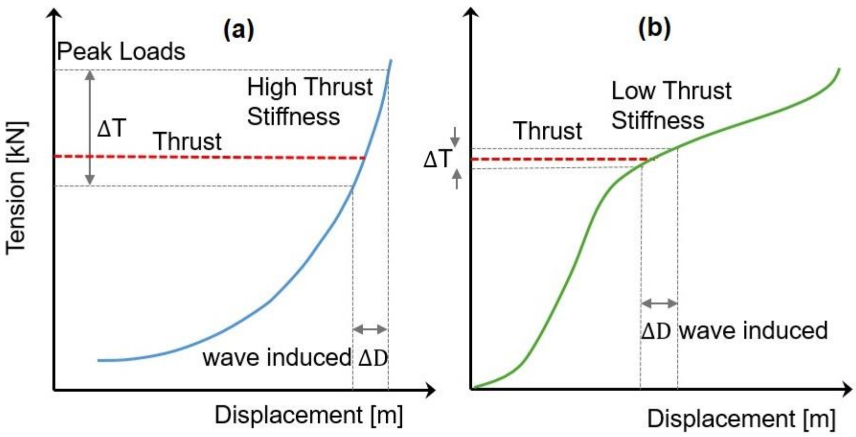

Figure 1. Qualitative Mooring line axial stiffness curve, (a) Chain-synthetic line, (b) Incorporating a LRDs.

2 Optimization framework

The optimization framework in this study follows a similar approach to that used by West et al. [6], employing the Non-Sorted Genetic Algorithm II (NSGA2) to find a Pareto Frontier for two competing objectives: minimizing cost and mooring system radii. However, this paper adopts a penalty-free niched approach, eliminating the need for penalty parameters [18]. The running metric, introduced by Blank and Deb [19], is used as a termination criterion to evaluate runs when the true Pareto front is unknown.

2.1 Definition of the optimization problem and objective functions

West et al. [6] note the unclear relationship between the mooring system and cost, emphasizing the importance of understanding it. To ensure competitive objectives, the mooring system radius and cost are mapped into competing criteria according to the eq. (1) and (2). Detailed explanations of this approach can be found in West et al. [6].

$$L(\boldsymbol{x}) = \sqrt{\left({C(\boldsymbol{x})}/{M_{norm}}\right)^2 + (R - R_{min})^2} \tag{1}$$

$$\varphi(\boldsymbol{x}) = tan^{-1}\left(\frac{R - R_{min}}{{C(x)}/{M_{norm}}}\right) \tag{2}$$

The optimization problem, including constraints, follows West et al. [6] and is illustrated in the eq. (3).

$$\begin{gathered} Maximize - L(\boldsymbol{x}) \ and \ \varphi(\boldsymbol{x}) \\ Subject \ to \ g_i(\boldsymbol{x}) \geq 0, i = 1,2, \ldots 8 \\ R_{min} \leq R \leq R_{max} \\ L_{syn_{min}} \leq L_{syn} \leq L_{syn_{max}} \\ L_{spr_{min}} \leq L_{spr} \leq L_{spr_{max}} \\ D_{chain_{min}} \leq D_{chain} \leq D_{chain_{max}} \\ D_{syn_{min}} \leq D_{syn} \leq D_{syn_{max}} \\ V_{min} \leq V \leq V_{max} \\ TL_{min} \leq TL \leq TL_{max} \end{gathered} \tag{3}$$

wherein the symbols are illustrated in Tab.1.

2.2 Design variables

Table 1 illustrates the design variables and their range of definition.

Table 1. Design variables

Design variable	Description	Variable Type	Range
R	Mooring system radius	Continuous	250 m – 400 m
L_{syn}	Length of the nylon line (as fraction of radius)	Continuous	0.4 - 0.61 (100 m – 244 m)
L_{spr}	Length of the spring (as fraction of radius)	Continuous	0.02 - 0.04 (5 m – 16 m)
d_{syn}	Diameter of the nylon line	Continuous	175 mm – 240 mm
d_{chain}	Diameter of the chain line	Continuous	135 mm – 178 mm
V	Buoy displaced volume	Continuous	0 m^3 – 10 m^3
TL	Target load of the spring component	Continuous	3000 (kN) – 6000 (kN)

2.3 Constraints

The constraints used are as follows: $g_1(\boldsymbol{x})$ is the mooring system geometric constraint, $g_2(\boldsymbol{x})$ is the platform heave natural period constraint, $g_3(\boldsymbol{x})$ is the platform pitch natural period constraint. $g_4(\boldsymbol{x})$ is the platform surge natural period constraint, $g_5(\boldsymbol{x})$ is the synthetic touchdown constraint, $g_6(\boldsymbol{x})$ is the time-domain chain ultimate strength constraint. $g_7(\boldsymbol{x})$ is the time-domain synthetic ultimate strength constraint. Detailed descriptions and mathematical formulations for these constraints are not included here due to space limitations and can be found in West et al.[6]. For the mooring system integrating the spring polymer, another constraint is added as formulated in the eq. (4):

$$\begin{gathered} if \ Tension_{fairlead_{max}} \geq TL: \\ Then \ g_8 = 3\,\frac{Tension_{fairlead_{max}} - TL}{TL} \\ Else: g_8 = 0 \end{gathered} \tag{4}$$

3 Input data

The mooring system configuration, the characteristics of the floating turbine, the design requirements and environmental condition can be found in West et al.[6] The additional characteristics of the mooring system integrating the spring are modeled in OrcaFlex using the eq. (5) and the Tab.2:

$$c = \frac{TL}{2500} \tag{5}$$

Table 2. Look-up table varying with Target Load.

Elongation [%]	0	5	10	15	20	25	30	35	40	45	46.5	50
Tension [kN] x10^2	c*0	c*5	c*9	c*12	c*16	c*19	c*21	c*22	c*24	c*25	c*26	c*32

The linear mass of the spring was estimated using data from Lozon et al. [8], where a spring with a target load of 4000 kN has a linear mass of 1759.9 [kg/m]. The spring's linear mass is estimated by scaling the linear mass of the polymer spring with a target load of 4000 kN, according to the eq. (6):

$$linear\ mass = \frac{1759.9}{4000} TL \tag{6}$$

The cost of the spring component was sourced from McEvoy et al. [17], who estimated the spring's price to be 20% higher than that of the chain. The spring price is detailed in Tab.3.

Table 3. Spring Cost component.

Material	**Cost (USD/kg)**
Spring component	1.5*1.2 = 1.8

4 Modelling approach to approximate the maximum load

The ABS-recommended method utilizes quasi-static stiffness to determine the system's pretension and calculate both the mean offsets of the platform and the tensions in the mooring lines [20]. For dynamic simulations, dynamic line stiffness is applied, and the initial line length is adjusted to match the pretension derived from the quasi-static stiffness used in static simulations. Once the pretension alignment is achieved, dynamic simulations are conducted using dynamic stiffness. Response amplitudes from these simulations are then added to the mean tension obtained from the static simulations. A random design underwent six 1-hour simulations each with different seed according to ABS guidelines to compute the average maximum tension, accounting for wave loads and the mean loads of drift wave, current, and wind as per the approach proposed by West et al.[6]. Following this, 24 simulations of 1000 seconds each with different seeds were performed. Maximum tension peaks were fitted to a generalized extreme value (GEV) distribution to extrapolate the maximum tension with higher probability. The seed -1298747991, which best matched the extrapolated tension to the average tension, was selected. For a detailed illustration of the method see West at al.[15].

5 Results

The optimization framework proposed by West et al.[6] is enhanced using a design of experiment approach to identify the design variables that most significantly influence line tension load. A comparison is then made between the optimization using all variables and the optimization using only the most important variables.

5.1 Design of experiment

A random design is selected, with lower and upper levels calculated by adding ±10% to their values. A full factorial design matrix is generated, followed by 2^7 OrcaFlex simulations to calculate the tension load in line using the approximated approach. An ANOVA analysis identifies the most influential design variables: radius, line length, spring length, nylon diameter, and target load, as illustrated in Tab.4. The results of this sensitivity analysis for spring length and target load are also supported by the findings of Festa et al. [21]. It also presents interactions between variables up to the 3rd order, revealing that the interaction between the buoy volume, and other variables is not statistically significant ($p < 0.05$), though these interactions are not shown here for brevity. For details about this approach see the work of Ferreira et al. [22].

Table 4. ANOVA

Source of variation	Sum of Squares	Degree of freedom	F	P(>F)	Significance
Radius	4.64E+09	1	1091292	3.8E-137	P < 0.05
Line length	1.95E+09	1	459069.9	4.1E-125	P < 0.05
Spring length	37054493	1	8708.035	4.14E-70	P < 0.05
Chain diam	663057.7	1	155.8227	8.33E-19	P < 0.05
Nylon diam	1.92E+08	1	45136.22	6.77E-93	P < 0.05
Buoy volume	0.228863	1	5.38E-05	0.994171	
Target Load	1514485	1	355.9133	7.74E-28	P < 0.05

5.2 Optimization

The NSGA2 optimization framework was executed using Pymoo's default values, as detailed in Tab.5. For the optimization involving six design variables, the population size was proportionally reduced. The excluded design variable, buoy volume, was kept constant, 1.5 m^3. Notably, this less influential design variable converged to this value during the optimization involving all seven variables. The simulation time was 156 hours for the seven design variables and 120 hours for the six design variables. Running the 2^7 time-domain simulations for the DOE took about 2 hours, resulting in a total time of 122 hours for the DOE and optimization framework using the four design variables.

Table 5. Parameters for the NSGA2

Parameter	Value
Population size (7 design variables)	140
Population size (6 design variables)	120
Crossover operator	Exponential
Crossover probability	0.9
Crossover distribution index (η)	15
Mutation operator	Exponential
Mutation probability	0.9
Mutation distribution index (η)	20
Elitism	Implicit to NSGA2

The Pareto frontiers for both optimizations, shown in Fig.2, demonstrate good agreement. However, the 2^{nd} optimization narrowed the radii range. The Pareto frontier of the synthetic chain mooring system optimized by West et al. [6] presented costs ranging from $1.25 to $1.4 million, while the alternative system showed significantly lower costs ranging from $0.7 to $1 million. Table 6 indicates that the average Factor of Safety (FoS) of the solutions is slightly higher than the target FoS, suggesting that the chain and nylon diameters can be further reduced. However, the algorithm is unable to select smaller diameters due to the fixed lower bound values for the chain and nylon.

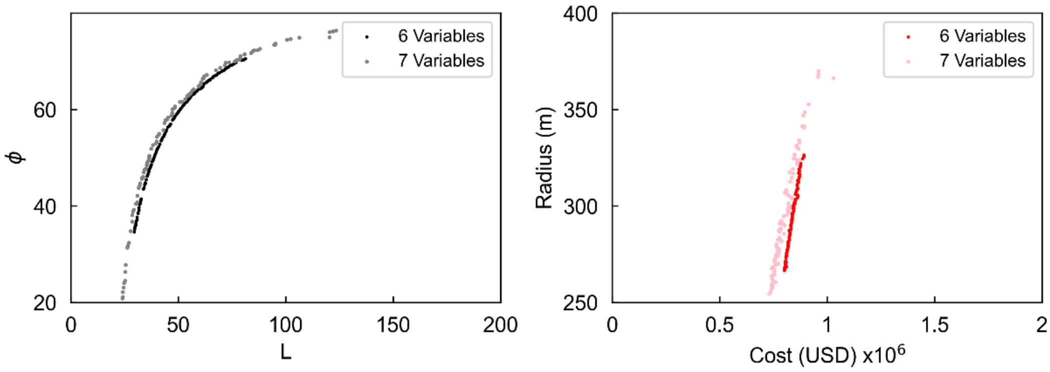

Figure 2. Objective Space

Table 6. Factor of Safety (FoS) statistic

Design Variables	Material	Target FoS	Average FoS	Max FoS	Min FoS	FoS COV
7	Chain	3.30	3.47	3.90	3.38	2.21%
	Synthetic	2.18	2.23	2.35	2.18	1.63%
6	Chain	3.3	3.48	3.58	3.58	1.19%
	Synthetic	2.18	2.24	2.31	2.18	1.22%

6 Conclusions

The optimization framework developed by West et al. [6] is applied to an innovative mooring system using a LDR in the form of a polymer spring. This framework is enhanced by incorporating a design of experiment (DOE) approach to identify and exclude design variables that do not significantly influence tension load calculation, which is crucial for determining solution feasibility. By reducing the design variables, the population size can be proportionally decreased, cutting computational time by up to 22% while still achieving a satisfactory Pareto frontier in a narrowed radii range. The Pareto frontiers in both the mapped and original spaces show good agreement and significant cost reductions compared to a more traditional synthetic chain mooring system. Additionally, the Factor of Safety (FoS) statistics from both optimizations suggest the potential for further reducing the chain and nylon diameters, thereby lowering costs. An important limitation is that the second optimization narrowed the range of radii, and the trade-off between this drawback and the time savings must be carefully evaluated. A more critical limitation is that, since the method relies on mean loads from drift waves, currents, and wind while considering design load case (DLC) 6.1, any selected design solution must undergo a complete suite of DLCs, incorporating time series analyses of drift wave, current, and wind loads to ensure comprehensive validation. Further research could explore the use of advanced probabilistic surrogate-assisted frameworks for constrained multi-objective or many-objective optimization, along with the inclusion of additional DLCs, such as those related to the fatigue limit state.

Acknowledgements. The authors thank the LCCV of the Federal University of Alagoas and Orcina LTD for their technical support. The third author acknowledges the support from the Brazilian National Council for Scientific and Technological Development (CNPq) to develop this work.

Authorship statement. The authors hereby confirm that they are the sole liable persons responsible for the authorship of this work, and that all material that has been herein included as part of the present paper is either the property (and authorship) of the authors or has the permission of the owners to be included here.

References

[1] R. Williams, A. Martinez Palacio, and F. Zhao, “GLOBAL OFFSHORE WIND REPORT.” Accessed: Jan. 24, 2024. [Online]. Available: https://gwec.net/wp-content/uploads/2023/08/GWEC-Global-Offshore-Wind-Report-2023.pdf

[2] Gov.br, “Portal vai unificar tramitação de empreendimentos de energia offshore.” Accessed: Jan. 24, 2024. [Online]. Available: https://www.gov.br/pt-br/noticias/energia-minerais-e-combustiveis/2022/10/portal-vai-unificar-tramitacao-de-empreendimentos-de-energia-offshore

[3] Empresa de Pesquisa Energética, “Roadmap Eólica Offshore Brasil.” Accessed: Jan. 24, 2024. [Online]. Available: https://www.epe.gov.br/sites-pt/publicacoes-dados-abertos/publicacoes/PublicacoesArquivos/publicacao-456/Roadmap_Eolica_Offshore_EPE_versao_R2.pdf

[4] A. C. Pillai, T. J. Gordelier, P. R. Thies, D. Cuthill, and L. Johanning, “Anchor loads for shallow water mooring of a 15 MW floating wind turbine—Part II: Synthetic and novel mooring systems,” *Ocean Engineering*, vol. 266, Dec. 2022, doi: 10.1016/j.oceaneng.2022.112619.

[5] S. Verde and E. N. Lages, “A comparison of anchor loads, planar displacement, and rotation for nylon and polyester moored systems for a 15 MW floating wind turbine in shallow water,” *Ocean Engineering*, vol. 280, Jul. 2023, doi: 10.1016/j.oceaneng.2023.114404.

[6] W. M. West, A. J. Goupee, S. T. Hallowell, and A. M. Viselli, “Determination of minimum-cost synthetic mooring systems for large floating wind turbines deployed in intermediate water depths,” *Journal of Renewable and Sustainable Energy*, vol. 15, no. 1, Jan. 2023, doi: 10.1063/5.0123474.

[7] I. Aryawan, P. McEvoy, S. Kim, and R. P. Faria, “Potential Mooring System Optimization Using Polymer Spring Component – Floating Offshore Wind Turbine Application,” in *Proceedings of the Annual Offshore Technology Conference*, Offshore Technology Conference, 2023. doi: 10.4043/32410-MS.

[8] E. Lozon, M. Hall, P. Mcevoy, S. Kim, and B. Ling, “Design and Analysis of a Floating-Wind Shallow-Water Mooring System Featuring Polymer Springs. In: ASME 2022 4th International Offshore Wind Technical. Ocean, Offshore and Arctic Engineering Division.,” 2022. doi: 10.1115/IOWTC2022-98149.

[9] G. Benassai, A. Campanile, V. Piscopo, and A. Scamardella, “Optimization of Mooring Systems for Floating Offshore Wind Turbines,” *Coastal Engineering Journal*, vol. 57, no. 4, Dec. 2015, doi: 10.1142/S0578563415500217.

[10] M. Brommundt, L. Krause, K. Merz, and M. Muskulus, “Mooring system optimization for floating wind turbines using frequency domain analysis,” in *Energy Procedia*, Elsevier Ltd, 2012, pp. 289–296. doi: 10.1016/j.egypro.2012.06.111.

[11] L. Li, Z. Jiang, M. C. Ong, and W. Hu, “Design optimization of mooring system: An application to a vessel-shaped offshore fish farm,” *Eng Struct*, vol. 197, Oct. 2019, doi: 10.1016/j.engstruct.2019.109363.

[12] F. M. G. Ferreira, E. N. Lages, S. M. B. Afonso, and P. R. M. Lyra, “Dynamic design optimization of an equivalent truncated mooring system,” *Ocean Engineering*, vol. 122, pp. 186–201, 2016, doi: 10.1016/j.oceaneng.2016.06.021.

[13] NREL, “OpenFAST Documentation Release v2.3.0,” 2020, *National Renewable Energy Laboratory, Golden, CO, USA.*

[14] M. Hall, “MoorDyn User’s Guide,” 2015, *Orono, ME, USA.*

[15] W. West, A. Goupee, S. Hallowell, and A. Viselli, “Development of a Multi-Objective Optimization Tool for Screening Designs of Taut Synthetic Mooring Systems to Minimize Mooring Component Cost and Footprint,” *Modelling*, vol. 2, no. 4, pp. 728–752, Dec. 2021, doi: 10.3390/modelling2040039.

[16] P. Mcevoy and S. Kim, “Mooring load management for SR2000 floating tidal device using non-linear polymer components.,” 2017. Accessed: Sep. 28, 2023. [Online]. Available: https://uploads-ssl.webflow.com/5f8964a5a533790d6cc8820a/5f96cb7a8ba32845a778cb9e_EWTEC-2017.pdf

[17] P. McEvoy, E. Johnston, and T. Marine, “Polymer Mooring Component for Offshore Renewable Energy. In Offshore Technology Conference.,” Houston, Texas, USA, 2019. doi: 10.4043/29587-MS.

[18] K. Deb and S. Agrawal, “A Niched-Penalty Approach for Constraint Handling in Genetic Algorithms,” in *Artificial Neural Nets and Genetic Algorithms.*, Vienna.: Springer, 1999. doi: 10.1007/978-3-7091-6384-9_40.

[19] J. Blank and K. Deb, “A Running Performance Metric and Termination Criterion for Evaluating Evolutionary Multi-and Many-objective Optimization Algorithms.,” in *IEEE Congress on Evolutionary Computation (CEC).*, Glasgow, UK.: IEEE, Jul. 2020. doi: 10.1109/CEC48606.2020.9185546.

[20] ABS, “Guidance Notes on the Application of Fiber Rope for Offshore Mooring.,” 2021, *ABS: Spring, TX, USA,.*

[21] O. Festa, S. Gourvenec, and A. Sobey, “Comparative analysis of load reduction device stiffness curves for floating offshore wind moorings,” *Ocean Engineering*, vol. 298, Apr. 2024, doi: 10.1016/j.oceaneng.2024.117266.

[22] F. M. G. Ferreira, E. N. Lages, S. M. B. Afonso, and P. R. M. Lyra, “Using design of experiments and design optimization to determine statically equivalent mooring system on truncated water depth,” *Journal of Offshore Mechanics and Arctic Engineering*, vol. 139, no. 4, Aug. 2017, doi: 10.1115/1.4036376.